

Influence of the substrate temperature on the structural, optical, and electrical properties of tin selenide thin films deposited by thermal evaporation method

N. Kumar¹, V. Sharma¹, N. Padha¹, N. M. Shah², M. S. Desai², C. J. Panchal^{*2}, and I. Yu. Protsenko³

¹ Department of Physics and Electronics, Dr. Ambedkar Road, University of Jammu, Jammu-180 006, Jammu and Kashmir State, India

² Applied Physics Department, Faculty of Technology and Engineering, M. S. University of Baroda, Vadodara-390 001, Gujarat State, India

³ Appl. Physics Dept., Faculty of Electronic and Information Technologies, Sumy State University, Ukraine

Received 15 July 2009, revised 1 October 2009, accepted 5 October 2009

Published online 9 October 2009

Key words tin selenide thin film, substrate temperature, XRD, SEM, transmission analysis.

PACS 68.37.Lp, 73.61.Jc, 78.40.Fy, 78.66.-w, 81.15.-z

Thin films of tin selenide (SnSe) were deposited on sodalime glass substrates, which were held at different temperatures in the range of 350–550 K, from the pulverized compound material using thermal evaporation method. The effect of substrate temperature (T_s) on the structural, morphological, optical, and electrical properties of the films were investigated using x-ray diffraction analysis (XRD), scanning electron microscopy (SEM), transmission measurements, and Hall-effect characterization techniques. The temperature dependence of the resistance of the films was also studied in the temperature range of 80–330 K. The XRD spectra and the SEM image analyses suggest that the polycrystalline thin films having uniform distribution of grains along the (111) diffraction plane was obtained at all T_s . With the increase of T_s the intensity of the diffraction peaks increased and well-resolved peaks at 550 K, substrate temperature, were obtained. The analysis of the data of the optical transmission spectra suggests that the films had energy band gap in the range of 1.38–1.18 eV. Hall-effect measurements revealed the resistivity of films in the range 112–20 Ωcm for films deposited at different T_s . The activation energy for films deposited at different T_s was in the range of 0.14 eV–0.28 eV as derived from the analysis of the data of low-temperature resistivity measurements.

© 2010 WILEY-VCH Verlag GmbH & Co. KGaA, Weinheim

1 Introduction

The IV–VI semiconducting narrow energy band-gap compounds attract considerable scientific attention due to their potential application in the field of solar energy conversion strategies, sensors, laser materials, thin films polarizer, and thermoelectric cooling materials [1]. Tin selenide (SnSe) is a IV–VI semiconducting compound that crystallizes in orthorhombic crystallographic structure (space group D_{2h}^{16}) whose atomic arrangement within the crystal resembles a severely distorted NaCl-type of structure [2]. The existence of the tightly bound double layers of tin and selenium atoms stacked along the crystallographic c-axis suggests the bonding between the layers being of the weak van der Waals type, which leads to a highly pronounced layered type of structure. Such a structural arrangement leads to a pronounced anisotropy for the physical properties of this compound, which makes it particularly appealing for the fabrication of solar cells, because of their higher chemical stability without passivity than other semiconductors, such as Si, GaAs, InP, and CdSe, which need special passivity procedures in order to avoid photocorrosion [3–4]. SnSe has numerous applications in memory switching devices, in holographic recording systems or as an anode material to improve lithium

* Corresponding author: e-mail: cjpanchal_msu@yahoo.com

diffusivity [5]. Owing to this, SnSe has been studied in the form of both single crystal and thin films [6–8]. Researchers investigated a number of methods to prepare SnSe thin films viz. atomic layer deposition [9], chemical bath deposition [10], vacuum evaporation [11], chemical vapor deposition [12], spray pyrolysis [13], electrodeposition [14], etc. Thermal evaporation of pulverized SnSe is a simple technique, whose attractive features are the convenience for producing large-area devices, low temperature growth, enable morphological, and film thickness controlled by readily adjusting the electrical parameters.

In the present work, SnSe thin films were grown on glass substrates, held at different substrate temperatures (T_s), by the thermal evaporation technique. We study here the effect of T_s on the structural, morphological, optical, and electrical properties of films.

2 Experimental

Preparation of films The SnSe thin films, studied in this work, were all grown on organically cleaned sodalime glass substrates, held at different T_s and at a base pressure of 10^{-5} mbar, from fine-grained pulverized SnSe powder (99.9 %), which was obtained from Alfa Aesar (USA). All films considered in this study were deposited on soda lime glass substrates with dimensions of approximately $76 \times 25 \times 1$ mm³. The quality of the substrate, prior to the growth of the thin film, is a crucial factor, which influences the material properties of the deposited thin films. Surface defects, such as scratches and dust on the substrate, have an adverse effect on the structural properties of the thin film. In order to obtain glass substrates with a high degree of chemical cleanliness, the following procedure of organic cleaning was used: 1. The glass substrates were rinsed in hydrogen peroxide to remove contaminants. 2. Substrates were then cleaned, in turn, under vapors of acetone, trichloroethylene, and methanol, respectively.

The rate of deposition was 0.3 nm/s and typical thicknesses of the films were 100 nm that were continuously monitored during the deposition using a quartz crystal thickness monitor DTM -101 (Hind Hi Vac., India). The substrate temperature was measured using chromel-alumel thermocouple, which was kept in good thermal contact with the substrate.

Characterization techniques The structural characterization of the films under investigation were carried out using an X-ray diffractometer (XRD), D-Max-III (Rigaku), in 2θ range of 20° - 60° , at a scan-rate of 0.05°s^{-1} , using Cu K α ($\lambda = 0.154$ nm) radiation. The surface morphology of the films was studied using a scanning electron microscope (SEM), JSM-5600 (JEOL), operated at 20 kV. The optical transmittance measurements were carried out with unpolarized light, at normal incidence, in the photon energy range of 0.8-2.5 eV, using the monochromator, CM110, photo detectors, and a lock-in amplifier, SR-530. The whole setup was automated using Lab View (Version 8.2). Hall-effect measurements setup having a source meter 2420-C (Keithley) and a 6½ digit multimeter 2000, (Keithley), was used for the electrical characterizations of the as-deposited SnSe thin films. Low-temperature resistivity measurements for the samples were carried out in a liquid nitrogen bath in the temperature range 80-330 K using Keithley Model 6517A programmable electrometer.

3 Results and discussion

Structural analysis The XRD profile of SnSe thin films deposited on glass substrate at different T_s is shown in figure 1. The prominent Bragg reflection is occurring at or around $2\theta = 30^\circ$ corresponding to (111) diffraction plane, along with three other very weak diffraction peaks viz. (113), (020), (203), which confirms the polycrystalline nature of the film. A similar preferred orientation of grains along the (111) plane in SnSe film was observed in the evaporated SnSe thin films by Bhatt et al. [15] and by Dang Tran Quan [16]. On the other hand, H. Chandra et al. [17] had observed (400) diffraction plane for films grown by flash evaporation technique and Teghil et al. [18] had reported orientation of grains along (011) and (200) crystallographic planes in the SnSe thin film prepared by laser ablation method. The various preferred orientation of grains reported for SnSe films deposited using different techniques indicate that the mode of deposition plays a decisive role on the growth structure of the films. The analysis of the diffraction patterns also suggests that the SnSe thin-film deposited at 550 K T_s has orthorhombic structure with lattice parameters $a = b = 0.429$ nm and $c = 0.523$ nm belonging to the D_{2h}^{16} space group while the d-value corresponding to the (111) prominent peak is determined to be 0.292 nm. The obtained d-values of film matches well with Joint Council of Powder

Diffraction Standards (JCPDS) data card [19]. Furthermore, it is observed that as T_s increases the intensity of the diffraction peaks increases and we get well-resolved peaks at 550 K substrate temperature. This could be linked with the grain-growth with increase in T_s . This point requires further investigation of the film's microstructure, which has been performed using SEM.

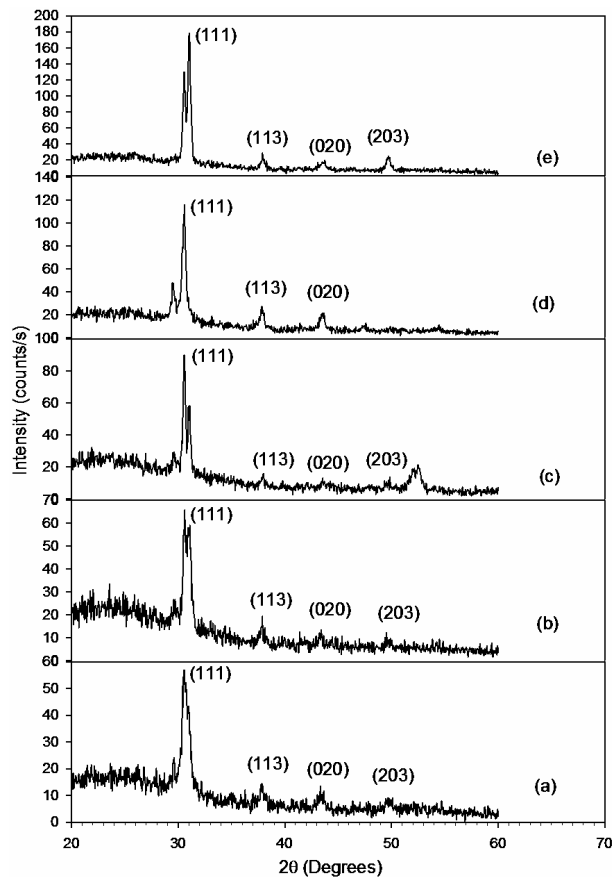


Fig. 1 The XRD Spectra of SnSe thin films for different substrate temperatures (T_s): (a) $T_s = 350$ K (b) $T_s = 400$ K, (c) $T_s = 450$ K (d) $T_s = 500$ K (e) $T_s = 550$ K.

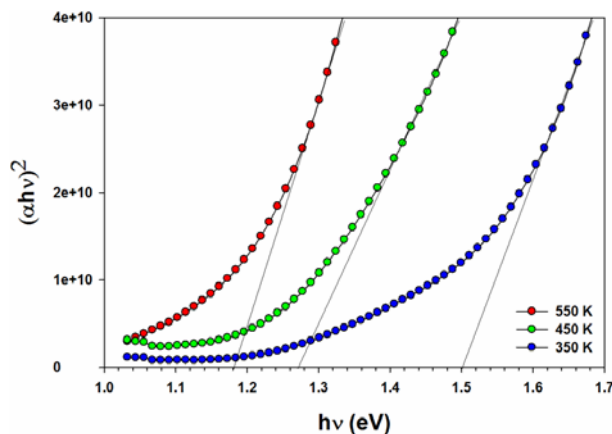


Fig. 3 Plots of $(\alpha h\nu)^2$ vs photon energy $h\nu$ for SnSe thin films deposited at (a) $T_s = 350$ K (b) $T_s = 450$ K (c) $T_s = 550$ K. (Online color at www.crt-journal.org)

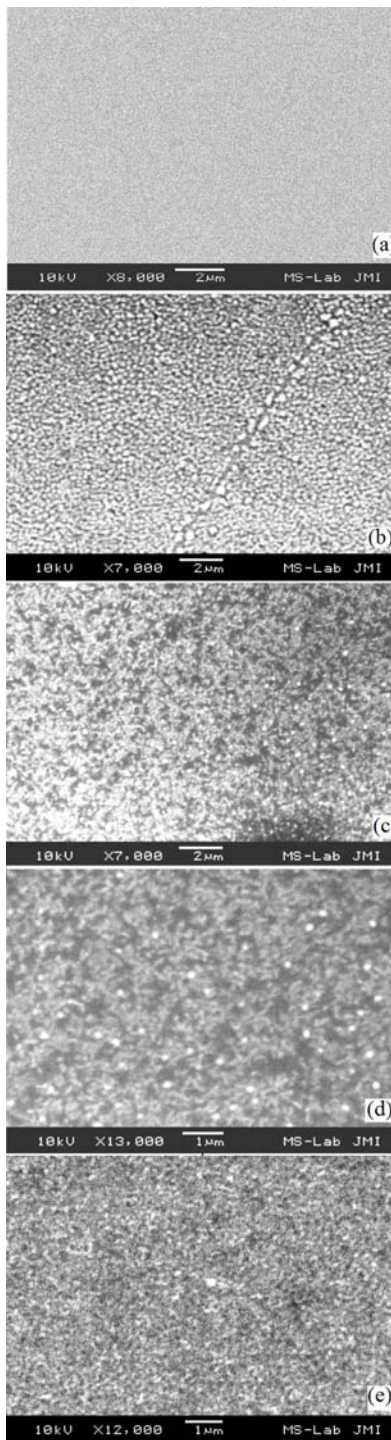


Fig. 2 The SEM images of SnSe thin films deposited at (a) $T_s = 350$ K (b) $T_s = 400$ K, (c) $T_s = 450$ K (d) $T_s = 500$ K (e) $T_s = 550$ K.

SEM analysis The microstructure of the thin films, deposited at different T_s , was investigated by the SEM to observe its surface topography. Figure 2 shows the SEM images of the synthesized SnSe thin films deposited at different T_s . The SEM micrograph shows that the grains are distributed to cover the surface of the substrate completely. No pinholes or cracks could be observed for the samples. It is also observed that with the increase in T_s the grain size increases while the density of the grains decreases. The increase in grain size with T_s indicates the increase in the crystallinity of the film. These results also corroborate the results obtained from the XRD data.

Optical analysis The transmission spectra of SnSe thin films, which were deposited at three different T_s , were recorded in the wavelength range of 500 nm to 1500 nm, at normal incidence. From these spectral data, the optical absorption coefficient, α , was calculated using Lambert's law:

$$\ln\left(\frac{I_0}{I}\right) = 2.303A = \alpha d, \quad (1)$$

where, A is the optical absorbance, d is the film thickness, I_0 and I are the intensities of the incident and the transmitted light, respectively. The absorption coefficient, α , was found to follow the relation,

$$\alpha hv = B(hv - E_g)^{1/2}, \quad (2)$$

where B is a constant, and E_g is the band gap energy. Plots of $(\alpha hv)^2$ versus the photon energy (hv), for films deposited at three different T_s viz. 350 K, 450 K and 550 K are shown in figure 3. The linearity of the above plots near the absorption edge indicates that the material is of the direct band gap. Hence, the energy-axis intercept of the linear part yields the energy band gap of SnSe thin films. The energy band gap of films deposited at three different T_s was in the range of 1.50-1.18 eV. These values are in good agreement with the band gap values as reported by other workers [20-23]. It is clear that as T_s increases the energy band gap decreases. The decrease in the direct band gap energy with increase in T_s can be explained using the fact that the crystallinity of the polycrystalline SnSe films improves with increasing T_s .

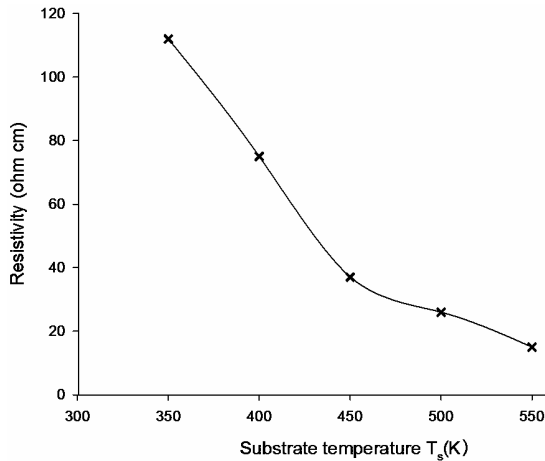


Fig. 4 The variation of the electrical resistivity of SnSe thin films deposited at different substrate temperatures, T_s .

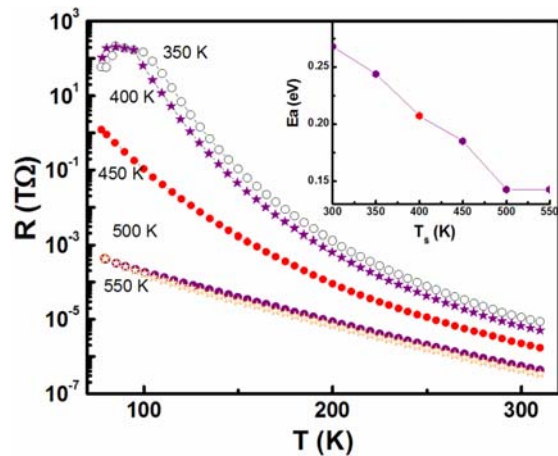


Fig. 5 Plots of the resistance (R) as a function of temperature (T) for SnSe thin films deposited at (a) $T_s = 350$ K, (b) $T_s = 400$ K, (c) $T_s = 450$ K, (d) $T_s = 500$ K, (e) $T_s = 550$ K. (Online color at www.crt-journal.org)

Resistivity measurement For all electrical measurements performed in this study, non-rectifying (ohmic) contact with the investigated films was achieved using silver-paste electrodes. The type of electrical conduction (p-type) in SnSe thin films was verified using the hot-probe method while the resistivity measurements were carried out using the standard Hall-effect setup. Figure 4 shows the variation of electrical resistivity with T_s . The decrease in resistivity with the increase in T_s can be explained using the Petritz barrier model: according to the model, the crystallites do not grow sufficiently large at low temperature and the larger inter-crystalline regions offer high resistance for the movement of the charge carriers. At high T_s , the formation of fewer nucleation centre results in large crystallite size, which may ultimately decrease the inter-crystalline barriers, hence decreasing the electrical resistivity. The resistivity values of SnSe films, deposited at different

T_s , varied between 112- 15 Ω and was strongly influenced by T_s . The value of the resistivity for the thin films deposited at 550 K is in close approximation to the value reported by H. Chandra et al. [17] for SnSe film deposited at 513 K T_s using the flash evaporation technique.

Activation energy The electrical conductivity of a polycrystalline thin film sample is a complex phenomenon, involving charge-carriers transport through both the “bulk-like” part of the semiconductor crystals and through the inter-crystalline (grain) boundaries.

In the literature [24] the temperature dependence of the semiconductor material’s conductivity is expressed by the equation

$$\sigma = \sigma_0 \exp\left(\frac{-E_a}{kT}\right) \quad (3)$$

where σ_0 is the pre-exponential factor, E_a is the activation energy for this thermally activated process and k is the Boltzmann constant. Clearly, a plot of $\ln(\sigma)$ versus $10^3/T$ will be a straight line, from the slope of which the activation energy can be calculated.

Thus, to measure the conductivity it is enough to measure the electrical resistance R since we are interested in the slope of the linear-least square fit only. So, the temperature dependence of resistance of SnSe thin films has been studied by measuring the resistance in the temperature range 80-330 K using the Keithley Model 6521 scanner card. Depending on the sample conductivity, a voltage limit was adjusted to obtain reliable data. The data collected was normally repeated for reproducibility check. After stabilizing to the desired temperature, the resistance values were normally recorded three times and their mean was noted. Once the dimensional factors were determined for each sample, the resistivity values were calculated. The resistivity thus obtained had an estimated error within 5%.

Figure 5 shows the plots of resistance versus temperature of SnSe thin films deposited at different T_s . The decrease in resistance with increase in temperature indicates semiconducting behavior of the thin films. The activation energies calculated from the linear-least square fit of the plots for SnSe thin films, deposited at different T_s , were in the range 0.14 eV-0.28 eV, which is also shown in-situ in the plot of the activation energy versus substrate temperature in figure 5. The values of the activation energy for electrical conduction closely correspond with the measurements performed by another group [25].

4 Conclusions

A simple thermal evaporation technique to deposit SnSe thin film at different substrate temperatures has been investigated. The structural and morphological analysis of the as-deposited films suggests that the thin films were polycrystalline in nature, having preferred orientation of grains along the (111) direction, and uniform distribution of grains at higher T_s . The direct energy band gap calculated from transmission data were in the range 1.50-1.18 eV. The high optical absorption in the visible region makes the thin films suitable to be used as a semitransparent layer in high-speed detectors working in the visible region and solar cell applications. Activation energy calculated from low temperature resistivity measurements were in the range 0.14 eV - 0.28 eV corresponding to shallow donor level near conduction band.

Acknowledgements C. J. Panchal and M. S. Desai are thankful to Department of Science and Technology, Government of India for financial assistance under INDO-UKRAINE program of cooperation in science and technology and I. Yu. Protchenko are thankful to Ministry of Education and Science of Ukraine, Ukraine for financial assistance

References

- [1] K. Zweibel, Sol. Energy Mater. Sol. Cells **63**, 375 (2000).
- [2] I. Lefebvre, M. A. Szymanski, J. Olivier-Fourcade, and J. C. Jumas, Phys. Rev. B **58**, 1896 (1998).
- [3] A. Aruchamy, Photoelectrochemistry and Photovoltaics of Layered Semiconductor (Kluwer Academic Publishers, Dordrecht, 1992) p. 101.
- [4] H. Tributsch, H. Gerischer, C. Clemen, and E. Bucher, Ber. Bunsenges. Phys. Chem. **83**, 655 (1979).
- [5] M. Z. Xue, J. Yao, S. C. Cheng, and Z. W. Fu, J. Electrochem. Soc. **153**, 270 (2006).
- [6] A. Agarwal, S. H. Chaki, and D. Lakshminarayan, Mater. Lett. **61**, 5188 (2007).
- [7] A. Agarwal, P. H. Trivedi, and D. Lakshminarayan, Cryst. Res. Technol. **40**, 789 (2005).

- [8] Z. Zainal, S. Nagalingam, A. Kassim, M. Z. Hussian, and W. M. M. Yunus, *Sol. Energy Mater. Sol. Cells* **81**, 261 (2004).
- [9] V. E. Drozd, I. O. Nikiforova, V. B. Bogevolnov, A. M. Yafyasov, E. O. Filatova, and D. Papazoglou, *J. Phys. D* **42**, 125306 (2009).
- [10] Z. Zainal, N. Saravanan, K. Anuar, M. Z. Hussein, and W. M. M. Yunus, *Mater. Sci. Eng. B* **107**, 181 (2004).
- [11] D. P. Padiyan, A. Marikani, and K. R. Murali, *Cryst. Res. Technol.* **35**, 949 (2000).
- [12] N. D. Boscher, C. J. Carmalt, R. G. Palgrave, and I. P. Parkin, *Thin Solid Films* **516**, 4750 (2008).
- [13] L. Amalraj, M. Jayachandran, and C. Sanjeeviraja, *Mat. Res. Bull.* **39**, 2193 (2004).
- [14] Z. Zainal, A. Jimale Ali, A. Kassim, and M. Z. Hussein, *Sol. Energy Mater. Sol. Cells* **79**, 125 (2003).
- [15] V. P. Bhatt, K. Gireesan, and C. F. Desai, *Cryst. Res. Technol.* **24**, 187 (1989).
- [16] D. T. Quan, *Phys. Status Solidi A* **86**, 421 (1984).
- [17] G. H. Chandra, J. Naveen Kumar, N. Madusudhana Rao, and S. Uthanna, *J. Cryst. Growth* **306**, 68 (2007).
- [18] R. Teghil, A. Santagata, V. Marotta, S. Orlando, G. Pizzella, A. Giardini-Guidoni, and A. Mele, *Appl. Surf. Sci.* **90**, 505 (1995).
- [19] Powder Diffraction File, Joint Committee on Powder Diffraction Standards, ASTM (1998) (Card no. 32-1392).
- [20] Z. Zainal, N. Saravanan, K. Anuar, M. Z. Hussein, and W. M. M. Yunus, *Mat. Sci. Eng. B* **107**, 181 (2004).
- [21] D. P. Padiyan, A. Marikani, and K. R. Murali, *Cryst. Res. Technol.* **35**, 949 (2000).
- [22] H. S. Soliman, D. A. Abdel Hady, and K. F. Abdel Chaudhuri, *Thin Solid Films* **165**, 257 (1988).
- [23] D. T. Quan, *Thin Solid Films* **149**, 197 (1987).
- [24] A. J. Moulson, *Electroceramics* (Wiley, USA, 1990), p. 26.
- [25] K. Chung, D. Wamwangi, M. Woda, M. Wuttig, and W. Bensch, *J. Appl. Phys.* **103**, 083523 (2008).